A Non-Inductive Bifilar Coil to Design Compact Flux Pumps for HTS Magnets

Muhammad H. Iftikhar, Jianzhao Geng, Weijia Yuan and Min Zhang

***Abstract*—High temperature superconducting flux pump is a promising way of energizing superconducting magnets without direct electrical contacts. It can remove the resistive heating and heat leakage from the current leads at room temperature. It is well known that applying the current over the critical current of the superconductor, will force the superconducting layer to enter into the flux flow regime. This flux flow resistivity generates a dc voltage across the length of the HTS tape. This phenomenon is well understood , however, it is difficult to generate a high dc charging voltage without a high current. In this work, we demonstrate a novel flux pumping technique by using a non-inductive bifilar bridge wound in parallel to the HTS coil. This configuration can generate large dc voltages using relatively small currents. It results in effectively pumping dc currents equal to the critical current for large HTS magnets.**

***Index Terms*—Flux pump, high current, HTS magnet, non-inductive bridge, persistent current operation, self-rectifier.**

I. Introduction

HIGH temperature superconducting (HTS) coated conductors (CC) exhibit high current carrying capability, good in-field performance as well as superior mechanical properties [1]. HTS magnet working in a persistent current mode (PCM) is an ideal candidate for using in high-field magnet systems [2], [3], e.g. magnetic resonance imaging (MRI) [4], nuclear magnetic resonance (NMR) [5] and superconducting motors [6], [7]. This predominantly stemmed from the fact that magnets constructed from HTS-CC are difficult to operate in the persistent current model due to relatively low n-values [8] and the lossless joint is hard to achieve [9], [10]. One way to overcome this problem is to operate a magnet using an external power supply, which will induce considerable heat losses due to copper leads transporting dc current from room temperature to cryogenic temperature [11]. These losses decrease system efficiency and increase cooling penalties. An alternative solution is to incorporate a flux pump. A flux pump device can inject a large dc current into a superconducting circuit without electrical contact [12]–[24]. HTS flux pumps are capable of charging the magnet and compensating for any current decay, enabling the quasi-persistent current operation of HTS-CC magnets. Various developments in HTS flux pumps have been documented recently, these flux pumps include travelling-magnetic field induced flux pumps (dynamo, linear) [14], [16], [25], and HTS rectifier flux pumps (thermal switching, dynamic resistance switching, JcB switching, self-switching, etc.) [18]–[20]. Researchers have concluded that in an HTS-CC when there is a flux motion a resistivity appears known as flux flow resistivity. This phenomenon of flux flow occurs when a superconductor is subjected to an ac field, transporting an ac current or transporting a dc current above its critical current. In [25] author proposed a self switched HTS flux pump, which works on the principle of driving the HTS-CC into the flux flow region in the *E-J* curve by injecting current above its critical current value. Numerous studies have been documented demonstrating flux pumping using this principle. These studies uses straight HTS tapes known as "the bridge" either single or parallel connected HTS tapes for passing high currents to achieve higher load currents. Following the principle presented by Geng et al. [25], in this paper, we demonstrated flux pumping using a non-inductive bifilar coil as a bridge. This configuration gives higher and stable dc voltages whilst the superconductor is subjected to a flux flow regime resulting in a higher load current. Moreover, a bifilar bridge leads to a compact size magnet with a bridge neatly wound across the magnet enabling it a substantial candidate for a complex applications like rotating machines.

A. Origin of DC Voltage in High Temperature Superconductor

When the transport current in a HTS superconductor exceeds the critical current value, the bridge is forced to enter into the flux flow regime. Which will generate a dc voltage across the bridge and can be given as;

$$v_{dc} = lV_c \left(\frac{i_b}{I_c}\right)^{n-1}, \tag{1}$$

Where l is length of the bridge, I_c is critical current of the bridge i_b is current flowing through the bridge and V_c is voltage criterion and n is the exponent of power law.

B. Non-Inductive Winding Structure

A coil constructed by two closely spaced, parallel wires is referred as non-inductive or a bifilar windings. Depending on the winding configuration it can be classified into three categories as illustrated in Figure 1. Series solenoid is a winding configuration in which the strands of wire are wound in parallel and the current flows in opposite direction in each wire. In the case of superconductors, it can be made by cutting an HTS tape as illustrated in Figure 1(a). However, this structure has its limitations; bulky size, relatively large

This work is supported by the Professor Min Zhang Royal Academy of Engineering Research Fellowship.

Muhammad Haseeb Iftikhar, Min Zhang and Weijia Yuan are with Applied Superconductivity Laboratory, Department of Electronics and Electrical Engineering, University of Strathclyde, Glasgow, G1 1XQ, United Kingdom. (email: min.zhang@strath.ac.uk).

Jianzhao Geng is with Wuhan National High Magnetic Field Center, Huazhong University of Science and Technology, Wuhan, 430074, China.

Manuscript received xx xx, xxxx; revised xx xx, xxxx.

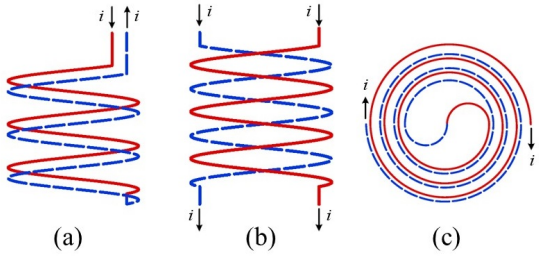

Fig. 1. Illustration of non-inductive coil structures; (a) series solenoid, (b) parallel solenoid, and (c) bifilar pancake.

impedance and ac losses. This configuration is used in making a fault current limiter (FCL) in Curl 10 project using BSCCO-2223 bulk [26]. Whereas, parallel solenoids have two adjacent coils in which the turns are arranged so that the potential difference is magnified. In a parallel solenoid, current flows in the same direction as illustrated in Figure 1(b). It can be realized to resolve the weak points of the series solenoid as well as bifilar pancake [27], [28]. A bifilar pancake is a simple winding configuration with compact size, small impedance, and low ac losses as in Figure 1(c). However, in this structure IN and OUT are insulated with only tape or paper which raises a high risk of electrical breakdown for high voltage applications. Applications like flux pumping require relatively low voltage so it rules out electrical breakdown potential risk. For example, to charge the load coil of 60kA in 24 hour, a dc voltage of 55mV is required and only 6mV is needed to maintain a long-term steady current of 60kA [29].

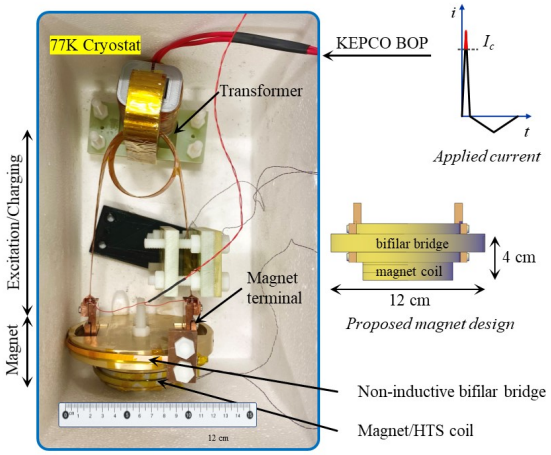

Fig. 2. Photograph of proposed flux pump, magnet is prepared by 4mm HTS tape in double pancake coil shape of diameter 75mm and the bifilar bridge is wound around the magnet with bridge geometry diameter 120mm. A transformer induces asymmetric current into the excitation circuit which is shorted with the bridge through copper terminals (magnet terminals). On the right-hand side applied current signal and schematic diagram of magnet are illustrated.

II. Methodology

An experiment test bench was built as shown in Figure 2, comprising a transformer as a source of flux, a bifilar coil as

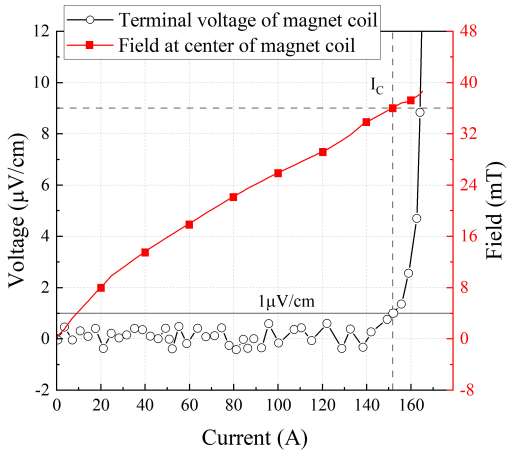

Fig. 3. Measured *V-I* curve for double pancake coil used as a load (magnet) in this experiment and its equivalent magnetic field measured at the center of the coil.

a bridge (source of a dc volage) and a HTS coil as the load. A 300:1 transformer was used with copper as the primary side, and the secondary side or the excitation coil, was built using HTS tapes with a critical of 600A. The ends of the excitation coil were connected to the HTS coil using a flux pump. The coil was built by winding a 6.8m long HTS tape into a double pancake coil. The magnet coil has an inductance of 0.6μH and the critical current at 77K with criterion E_o=10^{-4}Vm^{-1} was 152A, as shown in Figure 3 along with the magnetic field measured at its centre. The magnet coil is short-circuited by a 45cm long bridge made into a non-inductive bifilar coil configuration as illustrated in Figure 1(c). The magnet coil and the bifilar bridge together have a total diameter of 12 cm and height of 4 cm giving a compact geometry. This test bench is then compared with the flux pump configuration reported by Geng et al. [25]. The same excitation coil and the magnet coil mentioned earlier is used in this configuration. The only difference is with the bridge formation instead of a bifilar bridge a 30cm straighted HTS tape is used.

A KEPCO BOP 2010 power amplifier operated in current control mode was used to power the primary side of a transformer. An analogue voltage output module NI-9263 is used to control the power amplifier via LabVIEW. The primary current was measured using a 7.5 mΩ shunt resistor and the current in the excitation coil is measured using a pre-calibrated hall effect sensor. Another calibrated hall sensor is placed at the centre of the magnet coil to measure the coil's magnetic field. All signals are acquired using a NI-9238 card with a sampling rate of 1kHz. An equivalent circuit diagram of a conventional bridge based flux pump is shown in Figure 4(a) while the equivalent circuit of the proposed bifilar bridge based flux pump is presented in Figure 4(b). An equivalent primary current i_p is applied to the primary of the transformer in both cases. A proportional charging current i_s is induced in the excitation coil. A joint between the excitation coil and the magnet coil is represented by resistance R_s. Here the joint resistance has its significance, as it acts as

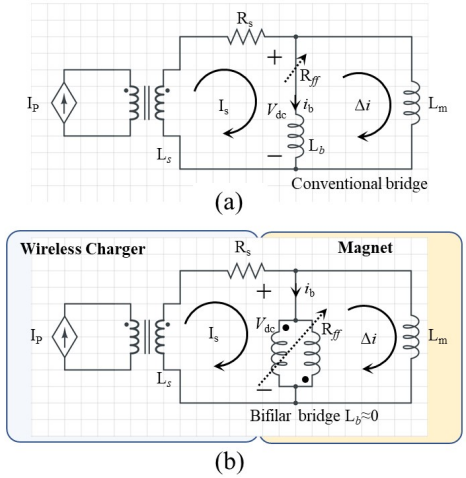

Fig. 4. Equivalent circuit model, (a) circuit diagram of flux pump with conventional bridge with flux flow resistivity R_{ff} and bridge inductance L_b, (b) circuit diagram of a flux pump with proposed bifilar bridge configuration where bridge inductance is cancelled out $L_b = 0$.

an essential component in flux pumping. It dumps down the dc component on the charging side, otherwise transformer core will be saturated. The origin of the R_{ff} (flux flow resistivity) is due to flux flow [30], whereas the inductance of the magnet coil is given by L_m.

III. Experiment and Results

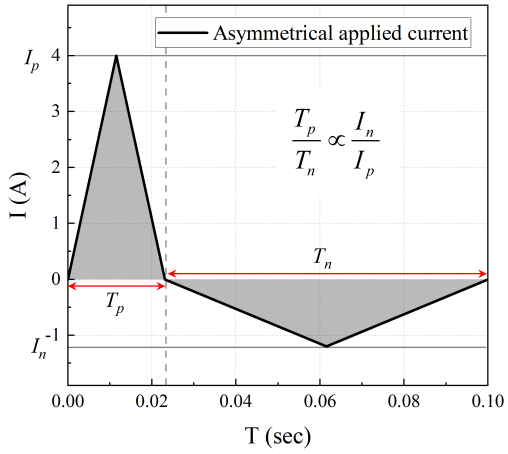

Fig. 5. An asymmetric applied current current waveform

A. Applied Current and Corresponding Induced Current

An asymmetric signal is applied as a primary (input) current signal in this experiment, presented in Figure 5. During the positive cycle, the current ramps to the positive peak I_p at a constant rate, and then damps down to zero at the same rate. Similarly, during the negative cycle, the current damps down to a negative peak I_n, then ramps up at the same rate to zero. The positive peak is kept higher to drive the superconductor into the flux flow region, enabling flux flow from the secondary

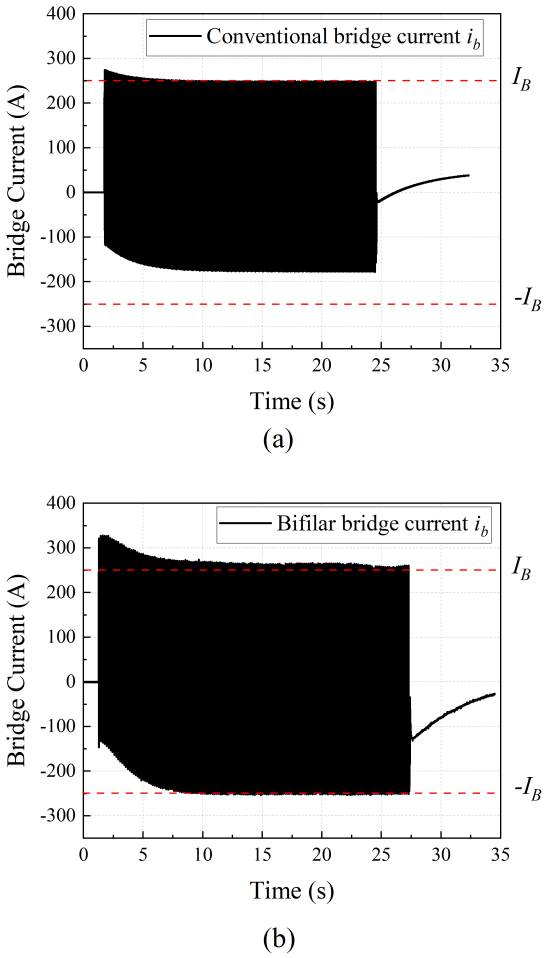

Fig. 6. The bridge current plot $i_b$ib, (a) the current flowing through the of conventional bridge, (b) the current flowing through the bifilar bridge.

side to the load side (magnet). However, the negative peak is kept at much lower values to retain the flux within the load. To make dc component zero, the length of the positive period over the negative period is kept inversely proportional to the peak values as;

$$\frac{T_p}{T_n} \propto \frac{I_n}{I_p}, \tag{2}$$

$$\int_0^T i_p\,(t)\,dt = 0, \tag{3}$$

Where, T_p is duration of positive peak, T_n is duration of negative peak, I_p is amplitude of positive peak, I_n is amplitude of negative peak, i_p is the primary current, and T, is time period. In both case primary current of amplitude 4A is applied to the primary of transformer as illustrated in Figure 5, which induces a charging current in the secondary side. The current induced in the excitation circuit can be mathematically derived using following equation.

$$0 = \frac{d\phi}{dt} + L_s\frac{di_s}{dt} + i_s R_s + i_s Z_b, \tag{4}$$

Where, ϕ is flux generated by primary copper of the transformer coupling with HTS excitation (secondary) coil, L_s is self inductance of excitation coil. i_s is excitation current, R_s is joint resistance and Z_b is bridge impedance.

B. Voltage Across the Bridge

For an ideal transformer action, the (secondary) charging current i_s is always proportional to its primary current i_p. However, for a real transformer, if the load impedance Z_b is high, the output voltage may reach its limit so that the secondary current cannot follow the primary current. A voltage limit for a transformer with HTS as a secondary can be stated as the voltage appears in a state when current above its critical current value flows through the HTS tape before quenching. In this section we will discuss the influence of the magnitude of applied current on the load current, since the bridge resistance originally depends on the primary current. If the peak value of the input current is kept relatively low to make bridge voltage reach the limit then the secondary current is proportional to the primary current with the transformer ratio. The bridge current i_b plot is illustrated in Figure 6. During the first cycle, the charging current will equal the bridge current because the load current (Δi) is zero. With the accumulation of load current, the bridge current will gradually be biased in the opposite direction. In this case, the dc voltage drops with the increase in the load current and it can be seen in Figure 7. Therefore the load current presents a curve similar to the charging curve of the first order circuit. When the applied current is too low to drive the bridge to the flux flow region, the load tends to saturates at a lower value. Keeping in mind the circuit diagram presented in Figure 4, a mathematical representation can be written as following;

$$i_s = i_b + \Delta i, \tag{5}$$

$$V_{dc} = i_b R_{ff} + L_b \frac{di_b}{dt} = L_m \frac{d\Delta i}{dt}, \tag{6}$$

Where V_{dc}, is the dc voltages across the bridge, in (6) for a bifilar bridge the L_b is zero so the dc voltages V_{dc} across the bridge is purely due to flux flow resistivity R_{ff}.

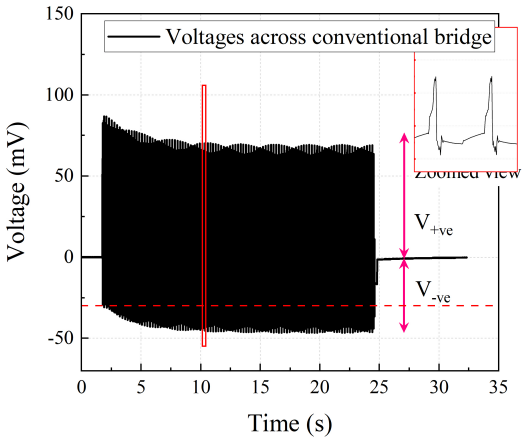

Fig. 7. The voltages measured across the conventional bridge in a flux pump.

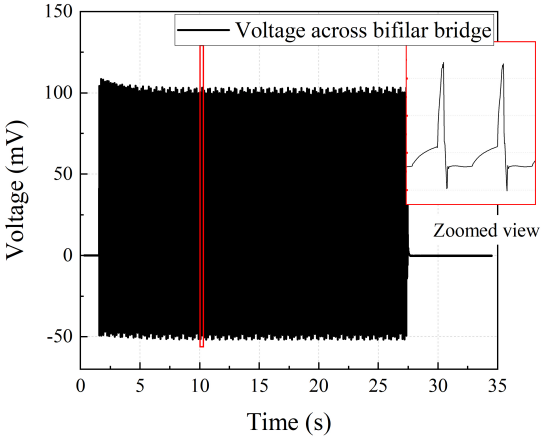

Fig. 8. The voltages measured across bifilar bridge in a flux pump.

In contrast, if the primary current level is too high, the bridge voltage will reach its limit. This means, that in each cycle bridge voltage will remain constant during the whole charging process and the load current increases by the same amount. The rate of change of the load current will be nearly constant in start and decrease as it will reach its critical current value. A bifilar bridge can induce a higher excitation current at a lower applied current due to negligible impedance offered by the bridge. It can achieve a voltage limit at a lower applied current. The dc voltages across the bifilar bridge is only due to the flux flow resitivity. By applying the input current of the same magnitude the dc voltage stays constant through the charging process. Hence, enabling flux pump to sufficiently charge the magnet coil to its critical current value. The measured bifilar bridge voltage plot is illustrated in Figure 8.

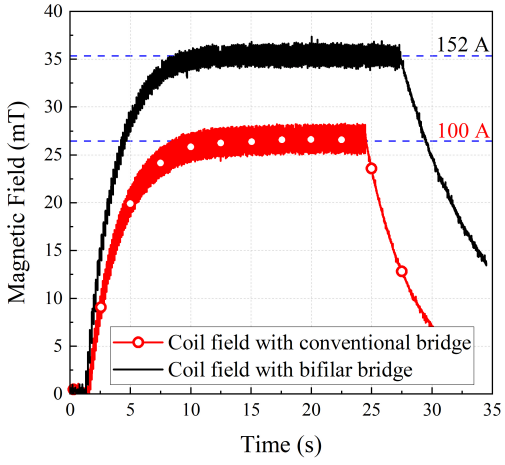

Fig. 9. The load's magnetic field measured at the center of the coil magnet for both cases, with conventional bridge saturating at 26mT and bifilar bridge at 35mT.

C. Flux Injection in Load Coil

The magnetic field plot of the coil magnet is illustrated in Figure 9, for both bridge configurations. A bifilar bridge can give a higher dc voltage to charge the magnet to its maximum capacity with minimal geometry. Whereas with the conventional bridge arrangement higher primary current is required to reach the voltage limit at the bridge to charge the coil to its critical current value. In section II it is already demonstrated that the critical current of the coil is 152A and at this value, it produces a magnetic field of 35mT at its centre. The mathematical relation between the bridge voltage V_{dc} and the load current can be given as;

$$\Delta i = \frac{1}{L_m} \int V_{dc} dt, \tag{7}$$

It is clear that using a bifilar bridge gives higher dc voltages. A comparison plot is illustrated in Figure 10, where the dc voltages and resultant magnetic field are plotted for both bifilar bridge and conventional bridge flux pump for the same applied current and magnet coil (load). The difference in the voltages can be seen as well as the change in the coil's field. In previous section, it is stated that if the peak value of the applied current is relatively low to make the bridge voltage reach limit. Then during charging with the gradual accumulation of dc current in the load, the bridge current is biased in the opposite direction and dc voltages on the bridge biased with the increase in the load current. Therefore, it contains both positive and negative components during a cycle as a result the rate of change of current decreases every cycle and the magnet will saturate before reaching its critical current. It is clearly illustrated in the magnetic field plot in Figure 10, that this negative component in the dc voltage is causing a rapid delay in the load current causing it to saturate at a lower value.

IV. Discussion

All previously reported self-switched HTS flux pump only needs a single transformer to achieve inductive flux transfer to a magnetic circuit. These flux pumps are suitable for quick pumping up currents in large magnets. The capacity of the transformer is the main limitation on the pumping speed of the flux pump. In terms of the field stability, however, these flux pumps may not be ideal. Because of the sharp *V-I* curve of the bridge superconductor, it is difficult to achieve effective control of the bridge voltage. A small noise in the bridge current may induce a large error in the bridge voltage. Previously this problem is solved by dynamic resistance control flux pumps [16], [17], which require an additional field source perpendicular to the bridge increasing the heat load on the cryogenic system and enlarging footprint. In contrast, the proposed flux pump with a bifilar bridge can induce higher voltages due to increased bridge length without adding inductance to the circuit. It not only gives higher but stable voltages at lower primary current

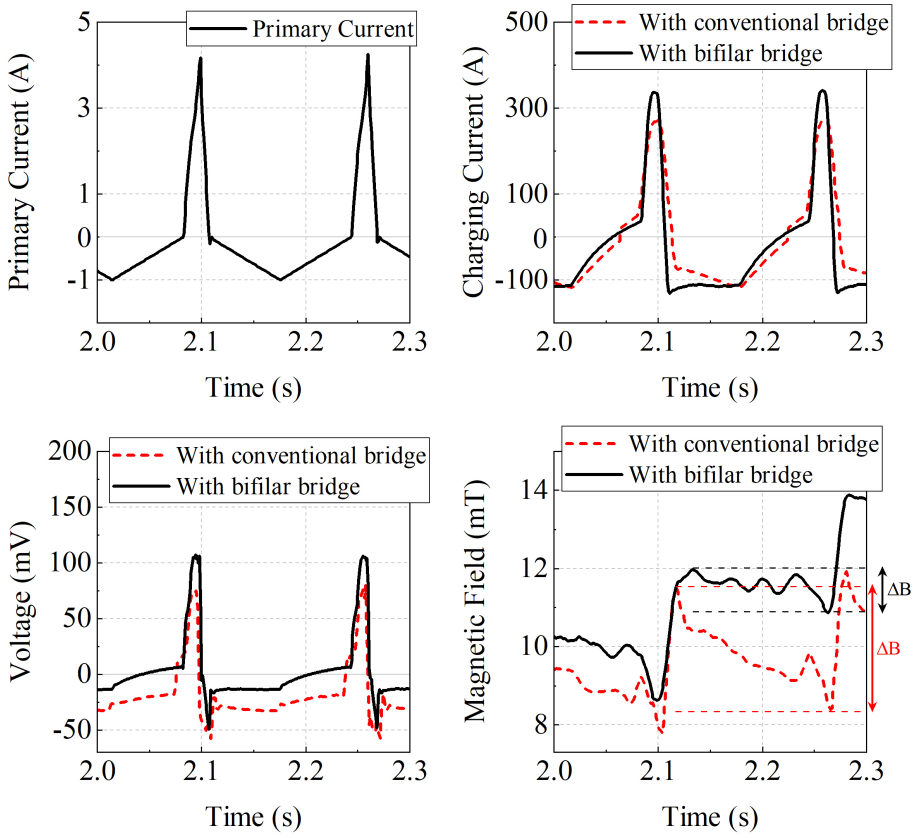

Fig. 10. Measured primary current, measured charging current for conventional and bifilar bridge, measured induced voltages across conventional and bifilar bridge and measured magnetic field in a magnet coil for conventional and bifilar bridge.

making it a constant voltage supply. It enables flux pumping at a stable dc voltages achieving persistent current operation in HTS magnets. A dc voltage of 100mV is required to charge the magnet of inductance 0.6μH to 152A, the total series resistance due to both HTS joint and the copper terminals of the magnet is 6.6E$^{-5}\Omega$.

The conventional bridge in a self switched HTS flux pump forms a loop whilst shorting the terminals of the magnets adding the inductance to the circuit. The length can be increased but with the increased length inductance also increases offering high impedance on the secondary side of the transformer. This impedance limits the flow of current on the primary side therefore it is difficult to achieve high charging current on the secondary side. By using the bifilar bridge the inductance in the bridge is eliminated and only flux flow resistivity exists, therefore high induced current in the excitation circuit and a stable voltage across the bridge can be achieved. A bifilar bridge also gives the freedom to adjust the length of the bridge depending on the voltage requirement of the load magnet. For example, in a cycle, with period T as shown in Figure 5, T_p is a flux pumping duration and T_n is flux decay duration. In a conventional bridge, the total impedance is higher compared to the bifilar bridge due to the inductive component therefore a rapid decay can be seen in the load's magnetic field as compared to the bifilar bridge configuration in Figure 10.

V. Conclusion

We have developed a compact HTS flux pump consisting of a transformer as a source of flux with a superconducting secondary winding, and a double pancake coil magnet which is shot-circuited by the non-inductive bifilar coil referred as "a bridge". The results show that the bifilar bridge gives higher and stable dc voltages (103mV) throughout charging time, when comparing to conventional HTS bridges. And it achieves the magnetic field of 35mT against the conventional bridge which saturates at 25mT with the same applied current. In a bifilar bridge configuration, the inductive component of the bridge is removed, so only flux flow resistivity generates a dc voltage across the bridge, allowing the HTS load to be charged effectively to its I_c value.

Acknowledgments

This work was funded by Prof. Min Zhang's Royal Academy of Engineering Research Fellowship. Muhammad H. Iftikhar acknowledges the John Anderson Research Award for offering a fully-funded studentship at the University of Strathclyde, Glasgow, United Kingdom.

References

[1] M. Sugano, K. Osamura, W. Prusseit, R. Semerad, T. Kuroda, K. Itoh, and T. Kiyoshi, "Reversible strain dependence of critical current in 100 a class coated conductors," *IEEE transactions on applied superconductivity*, vol. 15, no. 2, pp. 3581–3584, 2005.

[2] H. Weijers, U. Trociewitz, W. Markiewicz, J. Jiang, D. Myers, E. Hellstrom, A. Xu, J. Jaroszynski, P. Noyes, Y. Viouchkov *et al.*, "High field magnets with hts conductors," *IEEE transactions on applied superconductivity*, vol. 20, no. 3, pp. 576–582, 2010.

[3] Y. Iwasa, "Hts magnets: stability; protection; cryogenics; economics; current stability/protection activities at fbml," *Cryogenics*, vol. 43, no. 3-5, pp. 303–316, 2003.

[4] B. J. Parkinson, R. Slade, M. J. Mallett, and V. Chamritski, "Development of a cryogen free 1.5 t ybco hts magnet for mri," *IEEE transactions on applied superconductivity*, vol. 23, no. 3, pp. 4 400 405–4 400 405, 2012.

[5] R. M. Walsh, R. Slade, D. Pooke, and C. Hoffmann, "Characterization of current stability in an hts nmr system energized by an hts flux pump," *IEEE transactions on applied superconductivity*, vol. 24, no. 3, pp. 1–5, 2013.

[6] C. Y. Lee, J. H. Lee, J. M. Jo, C. B. Park, W. H. Ryu, Y. Do Chung, Y. J. Hwang, T. K. Ko, S.-Y. Oh, and J. Lee, "Conceptual design of superconducting linear synchronous motor for 600-km/h wheel-type railway," *IEEE transactions on applied superconductivity*, vol. 24, no. 3, pp. 1–4, 2013.

[7] Y. Jiang, R. Pei, W. Xian, Z. Hong, and T. Coombs, "The design, magnetization and control of a superconducting permanent magnet synchronous motor," *Superconductor Science and Technology*, vol. 21, no. 6, p. 065011, 2008.

[8] H.-S. Shin, K.-H. Kim, J. R. C. Dizon, T.-Y. Kim, R.-K. Ko, and S.-S. Oh, "The strain effect on critical current in ybco coated conductors with different stabilizing layers," *Superconductor Science and Technology*, vol. 18, no. 12, p. S364, 2005.

[9] Y. Kim, J. Bascuñán, T. Lecrevisse, S. Hahn, J. Voccio, D. K. Park, and Y. Iwasa, "Ybco and bi2223 coils for high field lts/hts nmr magnets: Hts-hts joint resistivity," *IEEE Transactions on Applied Superconductivity*, vol. 23, no. 3, pp. 6 800 704–6 800 704, 2013.

[10] Y. Park, M. Lee, H. Ann, Y. H. Choi, and H. Lee, "A superconducting joint for gdba2cu3o7- δ-coated conductors," *NPG Asia Materials*, vol. 6, no. 5, pp. e98–e98, 2014.

[11] A. Ballarino, "Current leads, links and buses," *arXiv preprint arXiv:1501.07166*, 2015.

[12] L. Van de Klundert and H. H. ten Kate, "Fully superconducting rectifiers and fluxpumps part 1: Realized methods for pumping flux," *Cryogenics*, vol. 21, no. 4, pp. 195–206, 1981.

[13] L. Van De Klundert and H. Ten Kate, "On fully superconducting rectifiers and fluxpumps. a review. part 2: Commutation modes, characteristics and switches," *Cryogenics*, vol. 21, no. 5, pp. 267–277, 1981.

[14] M. P. Oomen, M. Leghissa, G. Ries, N. Proelss, H.-W. Neumueller, F. Steinmeyer, M. Vester, and F. Davies, "Hts flux pump for cryogen-free hts magnets," *IEEE transactions on applied superconductivity*, vol. 15, no. 2, pp. 1465–1468, 2005.

[15] S. Ishmael, C. Goodzeit, P. Masson, R. Meinke, and R. Sullivan, "Flux pump excited double-helix rotor for use in synchronous machines," *IEEE transactions on applied superconductivity*, vol. 18, no. 2, pp. 693–696, 2008.

[16] J. Geng and T. Coombs, "Mechanism of a high-tc superconducting flux pump: Using alternating magnetic field to trigger flux flow," *Applied Physics Letters*, vol. 107, no. 14, p. 142601, 2015.

[17] J. Geng, K. Matsuda, L. Fu, B. Shen, X. Zhang, and T. Coombs, "Operational research on a high-tc rectifier-type superconducting flux pump," *Superconductor Science and Technology*, vol. 29, no. 3, p. 035015, 2016.

[18] Y. Chung, I. Muta, T. Hoshino, T. Nakamura, and M. Shon, "Design and performance of compensator for decremental persistent current in hts magnets using linear type magnetic flux pump," *Cryogenics*, vol. 44, no. 11, pp. 839–844, 2004.

[19] Z. Bai, G. Yan, C. Wu, S. Ding, and C. Chen, "A novel high temperature superconducting magnetic flux pump for mri magnets," *Cryogenics*, vol. 50, no. 10, pp. 688–692, 2010.

[20] L. Fu, K. Matsuda, and T. Coombs, "Linear flux pump device applied to hts magnets: further characteristics on wave profile, number of poles, and control of saturated current," *IEEE Transactions on Applied Superconductivity*, vol. 26, no. 3, pp. 1–4, 2016.

[21] C. Hoffmann, D. Pooke, and A. D. Caplin, "Flux pump for hts magnets," *IEEE Transactions on Applied Superconductivity*, vol. 21, no. 3, pp. 1628–1631, 2010.

[22] T. Coombs, J.-F. Fagnard, and K. Matsuda, "Magnetization of 2-g coils and artificial bulks," *IEEE Transactions on Applied Superconductivity*, vol. 24, no. 5, pp. 1–5, 2014.

[23] Z. Jiang, K. Hamilton, N. Amemiya, R. Badcock, and C. Bumby, "Dynamic resistance of a high-tc superconducting flux pump," *Applied Physics Letters*, vol. 105, no. 11, p. 112601, 2014.

[24] C. Bumby, Z. Jiang, J. Storey, A. Pantoja, and R. Badcock, "Anomalous open-circuit voltage from a high-t c superconducting dynamo," *Applied Physics Letters*, vol. 108, no. 12, p. 122601, 2016.

[25] J. Geng and T. Coombs, "An hts flux pump operated by directly driving a superconductor into flux flow region in the e–j curve," *Superconductor Science and Technology*, vol. 29, no. 9, p. 095004, 2016.
[26] R. Kreutz, J. Bock, F. Breuer, K.-P. Juengst, M. Kleimaier, H.-U. Klein, D. Krischel, M. Noe, R. Steingass, and K.-H. Weck, "System technology and test of curl 10, a 10 kv, 10 mva resistive high-tc superconducting fault current limiter," *IEEE transactions on applied superconductivity*, vol. 15, no. 2, pp. 1961–1964, 2005.
[27] T. Verhaege, C. Cottevieille, P. Estop, P. Therond, P. Thomas, Y. Laumond, M. Bekhaled, P. Bonnet, and V. Pham, "Investigations of hv and ehv superconducting fault current limiters," *IEEE Transactions on Applied Superconductivity*, vol. 5, no. 2, pp. 1063–1066, 1995.
[28] C. Lee, K. Nam, H. Kang, M. C. Ahn, T. K. Ko, and B.-Y. Seok, "Design of a high temperature superconducting coil for a 8.3 mva fault current limiter," *IEEE transactions on applied superconductivity*, vol. 17, no. 2, pp. 1907–1910, 2007.
[29] J. H. Rice, J. Geng, C. W. Bumby, H. W. Weijers, S. Wray, H. Zhang, F. Schoofs, and R. A. Badcock, "Design of a 60 ka flux pump for fusion toroidal field coils," *IEEE Transactions on Applied Superconductivity*, vol. 32, no. 4, pp. 1–5, 2021.
[30] H. Laquer, K. Carroll, and E. Hammel, "An automatic superconducting flux pump* *work performed under the auspices of the u.s. atomic energy commission." in *Liquid Helium Technology*, ser. Pure and Applied Cryogenics, vol. 6, pp. 539–544. Elsevier, 1966. [Online]. Available: https://www.sciencedirect.com/science/article/pii/B9780080124094500486

Muhammad Haseeb Iftikhar is pursuing his Ph.D. degree in electronic and electrical engineering with the University of Strathclyde, Glasgow, United Kingdom, before that he received his masters of engineering from University of Science and Technology, Daejeon, South Korea in 2019, and bachelor of science degree in electronics engineering from University of Engineering and Technology, Taxila, Pakistan in 2014. He was research student at Korea Electrotechnology Research Institute (KERI), South Korea from 2016 to 2019. His areas of research includes high temperature superconducting flux pumps and rectifiers, HTS magnets, motor drives and electric propulsion systems.

Jianzhao Geng received the B.E. degree in Electrical Engineering from the Huazhong University of Science and technology, Wuhan, China, in 2011, the M.S. degree in Electrical Engineering from Tsinghua University, Beijing, China, in 2014, and the Ph.D. degree in Engineering from the University of Cambridge, Cambridge, U.K., in 2017.,He was a Postdoc with the University of Cambridge until 2019. He currently holds a permanent position as a Professor at Wuhan National High Magnetic Field Center, Huazhong University of Science and Technology China. His main areas of research include the electromagnetism and applications of high-temperature superconductors, and power system protection and fault detection.

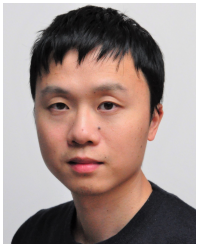

Weijia Yuan received his bachelor's degree from Tsinghua University in 2006 and his PhD from the University of Cambridge in 2010. He then became both a research associate in the Engineering Department and a junior research fellow at Wolfson College, both at the University of Cambridge, from 2010 to 2011. Yuan joined the University of Bath as a lecturer/assistant professor in 2011, where he was later promoted to reader/associate professor in 2016. He joined the University of Strathclyde as a professor in 2018. He is now leading a research team in the area applied superconductivity including energy storage, fault current limiters, machines, and power transmission lines.

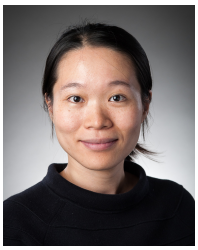

Min Zhang received her Ph.D. from the University of Cambridge in engineering. Before that, she received bachelor's and master's degrees from Tsinghua University in electrical engineering. Zhang spent a year as a Junior Research Fellow at Newnham College, Cambridge, and then joined the University of Bath as a lecturer. She joined the University of Strathclyde as a reader in 2018 and was promoted to Professor in 2021. Zhang's research focuses on the application of high temperature superconductors in power system transmission, renewable generation, and electric transportation..